



Primordial nucleosynthesis with decaying particles I. Entropy-producing decays

Robert J. Scherrer

Department of Physics
The University of Chicago
Chicago, Illinois 60637

Michael S. Turner

Theoretical Astrophysics
Fermi National Accelerator Laboratory
Batavia, Illinois 60510
and
Department of Astronomy and Astrophysics
The Enrico Fermi Institute
The University of Chicago
Chicago, Illinois 60637

ABSTRACT

We investigate the effect of a non-relativistic particle X, which decays out of equilibrium, on primordial nucleosynthesis, including both the energy density of the X particle and the electromagnetic entropy production from its decay. The results are parametrized in terms of the X particle lifetime τ and the density parameter rm_X , where m_X is the X particle mass, and r is the ratio of X number density to photon number density prior to nucleosynthesis. The results of primordial nucleosynthesis are given for $10^{-2} \text{ sec} \leq \tau \leq 10^7 \text{ sec}$, $10^{-2} \text{ MeV} \leq rm_X \leq 10^8 \text{ MeV}$, and $10^{-10.5} \leq \eta_f \leq 10^{-7.5}$, where η_f is the final baryon-photon ratio. It is shown that the primordial element abundances become independent of rm_X for sufficiently large values of rm_X . We give bounds on τ and rm_X which are valid for all values of η_f . For $rm_X \gtrsim 400\text{--}10^4 \text{ MeV}$, the upper bound on the particle lifetime is $\tau \lesssim 1\text{--}10 \text{ sec}$. Our results are applicable to any massive ($m_X \gtrsim 10 \text{ MeV}$), decaying particle which produces electromagnetic entropy in the course of its decay.



Primordial nucleosynthesis with decaying particles I. Entropy-producing decays

Robert J. Scherrer

Department of Physics
The University of Chicago
Chicago, Illinois 60637

Michael S. Turner

Theoretical Astrophysics
Fermi National Accelerator Laboratory
Batavia, Illinois 60510
and
Department of Astronomy and Astrophysics
The Enrico Fermi Institute
The University of Chicago
Chicago, Illinois 60637

ABSTRACT

We investigate the effect of a non-relativistic particle X, which decays out of equilibrium, on primordial nucleosynthesis, including both the energy density of the X particle and the electromagnetic entropy production from its decay. The results are parametrized in terms of the X particle lifetime τ and the density parameter rm_X , where m_X is the X particle mass, and r is the ratio of X number density to photon number density prior to nucleosynthesis. The results of primordial nucleosynthesis are given for $10^{-2} \text{ sec} \leq \tau \leq 10^7 \text{ sec}$, $10^{-2} \text{ MeV} \leq rm_X \leq 10^8 \text{ MeV}$, and $10^{-10.5} \leq \eta_f \leq 10^{-7.5}$, where η_f is the final baryon-photon ratio. It is shown that the primordial element abundances become independent of rm_X for sufficiently large values of rm_X . We give bounds on τ and rm_X which are valid for all values of η_f . For $rm_X \gtrsim 400\text{--}10^4 \text{ MeV}$, the upper bound on the particle lifetime is $\tau \lesssim 1\text{--}10 \text{ sec}$. Our results are applicable to any massive ($m_X \gtrsim 10 \text{ MeV}$), decaying particle which produces electromagnetic entropy in the course of its decay.

I. INTRODUCTION

One of the most powerful probes of conditions in the early Universe comes from primordial nucleosynthesis. The hot big bang seems to be the most likely site for the production of the observed ^2H , ^3He , ^4He , and ^7Li , and the predicted abundance of these elements is sensitive to the parameters governing their production in the early Universe (see the recent review of primordial nucleosynthesis by Boesgaard and Steigman 1985). One of these parameters is the expansion rate during nucleosynthesis, which depends on the energy density at early times ($t \sim 10^{-2} - 10^2$ sec). In general, the addition of "new" types of elementary particles beyond those included in the standard model for nucleosynthesis leads to a change in the energy density, altering the expansion rate and thereby changing the predicted light element abundances. A comparison of these predicted abundances with the observed light element abundances allows limits to be placed on new types of particles present during primordial nucleosynthesis (Shvartsman 1969; Steigman, Schramm, and Gunn 1977; Steigman, Olive, and Schramm 1979; Yang et al. 1979; Olive, Schramm, and Steigman 1981; Olive et al. 1981; Szalay 1981; Kolb and Scherrer 1982; Kolb, Turner, and Walker 1985; also the recent review by Boesgaard and Steigman 1985).

Previous studies have concentrated on particles which are stable throughout the era of nucleosynthesis, i.e., lifetimes $\gtrsim 100$ sec, but the effect of massive particles with lifetimes $\lesssim 100$ sec has not been addressed in a systematic way (although see Weinberg 1982). A massive particle species which decays out of equilibrium during nucleosynthesis alters the standard model in a far different way than a massive, stable particle species. In both cases, the expansion rate of the Universe during nucleosynthesis is increased, but any electromagnetic entropy produced by massive particle decays changes the time-temperature relationship in a different way and also dilutes the baryon-photon ratio, thereby requiring a larger initial baryon-photon ratio to obtain a given final baryon-photon ratio. (Electromagnetic entropy is defined as the total entropy of the photons and all relativistic particle species in thermal equilibrium with the photons). In a naive model, it might be thought that the massive particle decays would simply reheat the temperature to a sufficiently high value to allow the Universe to pass through nucleosynthesis again, with a new diluted baryon-photon ratio (see, for example, Weinberg 1982). However, it can be shown that particle decays which follow an exponential decay law can never increase the black-body temperature; they can only cause it to decrease less rapidly than in the standard model (Scherrer and Turner 1985a). Decay products can also photodissociate light nuclei produced during nucleosynthesis (Lindley 1979; for more recent discussions, see Lindley 1980, 1985; Scherrer 1984; Ellis, Nanopoulos, and Sarkar 1985). We do not consider this effect here and argue that it does not negate the limits which can be placed on the massive particle parameters on the basis of primordial nucleosynthesis alone (see Sec. IV).

In the following section, we discuss the parameters of interest: the massive particle lifetime (τ), the ratio of the massive particle energy density to the photon number density prior to the particle decay (rm_X), and the initial and final baryon-photon ratios (η_i and η_f). We also discuss our assumptions concerning the

particle decays. Although there are numerous particle physics theories which predict the existence of new particles, e.g., supersymmetric theories, we have attempted to keep our discussion as general as possible, and our results will be applicable to any particle which, in the course of its decay, produces electromagnetic entropy which is rapidly thermalized. Also in the next section we give a discussion of the time evolution of our parameters, and we discuss the conditions for which the time evolution of the Universe is a universal function of the particle lifetime.

In Section III we discuss our numerical calculations, including modifications to the standard model for primordial nucleosynthesis. Our results are given in Section IV, including constraints which can be placed on particle masses and lifetimes, and we then apply our results to two hypothetical particles: gravitinos and massive neutrinos. Our conclusions are summarized in Sec. V. In brief, we are able to rule out particle lifetimes $\gtrsim 1$ -10 sec for large values of rm_X ($rm_X \gtrsim 400$ - 10^4 MeV); our disallowed regions in the $\tau - rm_X$ plane are summarized in Fig. 9. In a companion paper (Scherrer and Turner 1985c) we address the question of a decaying particle which produces no electromagnetic entropy in the course of its decay ("inert" decays).

II. PRELIMINARIES

We assume a standard Friedmann-Robertson-Walker model with the expansion rate given by

$$H = \frac{\dot{R}}{R} = \left(\frac{8}{3}\pi G\rho\right)^{1/2}, \quad (1)$$

where ρ is the total energy density, and R is the cosmic scale factor. (At very early times the effect of curvature is slight and can be neglected). We have set the number of light two-component neutrino species at three and taken the neutron half-life to be 10.4 min. (Wohl et al. 1984, Bopp et al. 1984). The effect of altering the neutron half-life is discussed in detail by Olive et al. (1981). Changing these nominal values would affect the limits we derive only slightly. We take $\hbar = c = k = 1$ throughout.

The particle parameters of interest are the lifetime, τ , the particle mass, m_X , and the ratio of the particle number density to the photon number density prior to decay, r . We take $m_X \gtrsim 10$ MeV, so the massive particles are non-relativistic during nucleosynthesis, and $\tau \gtrsim 10^{-2}$ sec, so the particles are non-relativistic when they decay. We also assume that they follow a standard exponential decay law, i.e., the number of particles per comoving volume decreases exponentially. The ratio r is determined by the strength of the X particle coupling to the thermal background radiation. At sufficiently high temperatures, the X particles will be present in a thermal equilibrium concentration: $r \equiv n_X/n_\gamma = g_X/2$ if X is a boson, and $r = (3/4) g_X/2$ if X is a fermion, where g_X is the total number of spin degrees of freedom of the X particle. If the interaction rate of the X particles with the thermal background drops below the expansion rate while the X's are still relativistic ($T > m_X$), then the X particles will freeze out at the equilibrium concentrations given above. An example of this is the behavior of light or

massless neutrinos. On the other hand, if the X particles become non-relativistic while they are still in thermal equilibrium, then their concentration will be strongly suppressed by the Boltzmann factor, and the value of r when the X's drop out of thermal equilibrium will in general be much smaller than the values given above. In this case, an exact determination of r depends upon the annihilation cross section and requires an integration of the equations giving the time evolution of n_X (see, for example, Steigman 1979; Wolfram 1979; Scherrer and Turner 1985b). The value of r can change after the X's drop out of thermal equilibrium as the effective number of degrees of freedom in thermal equilibrium (g_*) changes; in the absence of entropy production, the entropy per comoving volume $R^3 g_* T_\gamma^3$ is constant, while $n_X \propto R^{-3}$ after freeze-out, so that at any time t after freeze-out,

$$\left(\frac{n_X}{n_\gamma}\right)_t = \left(\frac{n_X}{n_\gamma}\right)_{\text{freeze-out}} \left(\frac{g_{*t}}{g_{*\text{freeze-out}}}\right).$$

If there is entropy production after the X's drop out of equilibrium, e.g., due to a phase transition, then r decreases by the factor by which the entropy per comoving volume increases. In order to use a constant value for r , we define r to be the value of n_X/n_γ at a temperature T_0 and a time t_0 immediately prior to nucleosynthesis (chosen somewhat arbitrarily to be $T_0 \sim 10^{12} K$, with $g_*(T_0) = 43/4$), where we require the X's to be decoupled at this temperature, and the X's have not yet begun to decay ($t_0 \ll \tau$). The muon and pion degrees of freedom disappear at a time much earlier than the lifetimes of interest to us, so they have been ignored in this definition of r . If the X's were stable, then the value of n_X/n_γ today would simply be $\frac{4}{11}r$ due to entropy transfer from the disappearance of the e^+e^- pairs at a temperature of $O(0.1 \text{ MeV})$. The parameter which actually affects the time evolution of all of the quantities of interest is not n_X , but ρ_X . Therefore, since the X's are non-relativistic, r will enter into our calculations only in the combination rm_X :

$$rm_X \equiv \frac{n_X m_X}{n_\gamma} \Big|_{T_0 \sim 10^{12} K} = \frac{\rho_X}{n_\gamma} \Big|_{T_0 \sim 10^{12} K}. \quad (2a)$$

If ρ_{std} is the total energy density in the standard model during the radiation-dominated era, i.e., when nucleosynthesis takes place, then

$$\rho_X/\rho_{std} = 0.069 (rm_X/T_\gamma) \quad (2b)$$

prior to e^+e^- annihilation, and

$$\rho_X/\rho_{std} = 0.080 (rm_X/T_\gamma) \quad (2c)$$

after e^+e^- annihilation.

The other parameters which determine the results of primordial nucleosynthesis are η_i , the initial baryon-photon ratio before the X's decay, which of course is not an observable, and η_f , the final baryon-photon ratio after the decay of the X's. Barring any unforeseen physics, η_f is then the baryon-photon ratio today, which is in principle an observable. Baryogenesis calculations suggest an upper

limit to η_i (Kolb and Turner 1983):

$$\eta_i \lesssim 10^{-4}, \quad (3)$$

which we shall adopt here as an upper bound to η_i . The standard model for primordial nucleosynthesis gives very stringent limits on η_f , but these limits are obviously irrelevant here. The best direct limits on η_f come from observations of the luminous (and, therefore, presumably baryonic) parts of galaxies, which give a lower limit to η_f : $\eta_f \gtrsim 3 \times 10^{-11}$ (Faber and Gallagher 1979; Olive et al. 1981). Determinations of the cosmic deceleration parameter and the age of the Universe provide an upper limit to Ω_{TOTAL} : $\Omega_B h^2 \lesssim \Omega_{TOTAL} h^2 \lesssim 1$ (Freese and Schramm 1984; Steigman and Turner 1985). These bounds, to the nearest half order of magnitude, translate to

$$10^{-10.5} \leq \eta_f \leq 10^{-7.5}, \quad (4a)$$

or equivalently,

$$0.007 \lesssim \Omega_B \lesssim h^{-2}. \quad (4b)$$

The parameters η_i , η_f , τ , and rm_X are not independent; η_f is entirely determined by η_i , τ , and rm_X . We will be concerned primarily with the case in which the X decays produce a significant entropy increase ($\eta_f \ll \eta_i$), and we will assume that essentially all of the decay energy of the X particles goes into electromagnetic entropy production. The former condition will be satisfied as long as $\rho_X \gg \rho_r$ at the time of decay, where ρ_r is the energy density in relativistic particles in thermal equilibrium. An equivalent statement of this condition is

$$rm_X \gg T_D, \quad (5)$$

where T_D is the photon temperature when the X's begin to decay, i.e., at $t \approx \tau$. We derive a more exact expression below. The condition that all of the X decay energy go into electromagnetic entropy production does not imply that X's must decay into photons; any high-energy charged particle will yield its energy to the black-body background. This condition does imply, however, that most of the X decay energy not go into particles which interact only weakly, e.g., neutrinos. (This latter possibility is considered by Kolb, Turner, and Walker 1985). A discussion of the case in which the decaying X particle produces no electromagnetic entropy in the course of its decay will be given in a second paper (Scherrer and Turner 1985c). Finally, we assume that the X decay energy is thermalized and a black-body spectrum reestablished in a time much shorter than the expansion time scale. Any cases for which this is not a valid assumption can probably be ruled out, because the present-day microwave background is known to have a black-body spectrum to within a high degree of accuracy (Dicus, Kolb, and Teplitz 1978; Gunn et al. 1978).

With these assumptions, the final and initial entropy per comoving volume, S_f and S_i , are related by (Scherrer and Turner 1985a)

$$S_f/S_i = 0.36 \bar{g}_*^{-3/4} f_{e^+e^-} (rm_X/MeV) (\tau/sec)^{1/2}, \quad (6)$$

where \bar{g}_* is an average of the effective number of relativistic degrees of freedom in thermal equilibrium during the X decay (i.e., for $t \approx \tau$):

$$g_* = \sum (g_{boson} + \frac{7}{8} g_{fermion}), \quad (7)$$

and $f_{e^+e^-} = 1$ (if the decays occur prior to e^+e^- annihilation), $= 4/11$ (if the decays occur after e^+e^- annihilation). Eq. (6) differs from the expression given by Scherrer and Turner (1985a) by a factor of $\bar{g}_*^{-1} f_{e^+e^-}$ because of the different definition of τ , but the two expressions are exactly equivalent. Then

$$\eta_i/\eta_f = (11/4) S_f/S_i, \quad (8)$$

where 11/4 is the usual factor which arises from the annihilation of the e^+e^- pairs. A quantity of greater interest is the ratio $\epsilon \equiv \eta/\eta'$, where η' is the final baryon-photon ratio diluted by X decay, and η is the value that the baryon-photon ratio would have had in the absence of X decay:

$$\epsilon \equiv \eta/\eta' = S_f/S_i = 0.36 \bar{g}_*^{-3/4} f_{e^+e^-} (rm_X/MeV) (\tau/sec)^{1/2}. \quad (9)$$

For $\tau \geq 10^{-2}$ sec, g_* varies from 43/4 (photons, electron-positron pairs, and three pairs of neutrinos in equilibrium) to 2 (only photons in equilibrium), so $\bar{g}_*^{-3/4} f_{e^+e^-}$ varies from 0.17 to 0.28. The value of ϵ as a function of τ and rm_X (calculated numerically) is shown in Fig. 1.

We take $10^{-2} \leq \tau \leq 10^7$ sec; massive particles with lifetimes $\lesssim 10^{-2}$ sec decay too early to have any significant effect on primordial nucleosynthesis (we have verified this numerically), while entropy from the decay of particles with lifetimes $\gtrsim 10^7$ sec produces an unacceptable distortion in the black-body background, as the decay products do not thermalize completely (Dicus, Kolb, and Teplitz 1978; Gunn et al. 1978). We vary η_f within the range given by Eq. (4a); then the allowed values for rm_X are determined by the constraint on η_i (Eq. 3) and the relation between η_i and η_f given above. For sufficiently small values of rm_X , the X particle energy density during nucleosynthesis will not be large enough to significantly alter the expansion rate, so the final element abundances will be unaffected by the presence of the X particles. A stable particle with $rm_X < 0.1$ MeV has essentially no effect on the final element abundances, while large changes in the element abundances occur for $rm_X \gtrsim 1$ MeV. The question of precisely what value of rm_X is necessary to significantly alter the expansion rate during nucleosynthesis is therefore somewhat arbitrary; we have chosen the value $rm_X \sim 0.3$ MeV and indicated this in Fig. 1. The final element abundances for fixed η_f can still vary with rm_X when rm_X is below this limit, because η_i depends on rm_X for fixed η_f and τ .

It might seem that an arbitrarily large value of rm_X (or equivalently, an arbitrarily large increase in ρ_X at some fixed time prior to X decay) would produce a correspondingly large change in the time evolution of T and ρ_B (the baryon energy density) and thereby alter the results of nucleosynthesis to an arbitrary extent. However, it is possible to show that for sufficiently large rm_X , the time evolution of all of the parameters of interest and, therefore, the results of nucleosynthesis become completely independent of rm_X . The reason for this lies in the fact that the radiation energy density can be divided into a "new" component representing the radiation produced by the X decays, and an "old"

component representing the pre-existing radiation. Then rm_X enters only as a ratio between the X energy density and the "old" radiation at early times. Whenever the radiation energy density is dominated by the "new" component, and the expansion rate is dominated by either the X particle energy density or the "new" radiation energy density, then the evolution of all of the quantities which affect primordial nucleosynthesis becomes independent of rm_X .

More specifically, let $\rho_{r\ new}$ represent the radiation energy density produced by the X decays, and let $\rho_{r\ old}$ be the portion of the relativistic energy density which does not arise from the X decays. Then

$$\frac{d\rho_{r\ old}}{dt} = -4 H \rho_{r\ old}, \quad (10)$$

$$\frac{d\rho_{r\ new}}{dt} = -4 H \rho_{r\ new} + \Gamma \rho_X, \quad (11)$$

$$\frac{d\rho_X}{dt} = -3 H \rho_X - \Gamma \rho_X, \quad (12)$$

where Γ is the decay rate, $\Gamma \equiv 1/\tau$, H is given by Eq. (1):

$$H = \left[\frac{8\pi G}{3} (\rho_X + \rho_{r\ old} + \rho_{r\ new}) \right]^{1/2}, \quad (13)$$

and the contribution of ρ_B to the energy density can be neglected. Eqs. (10) and (11) are not strictly valid through the era of e^+e^- annihilation, but they will be sufficient for our purposes. Prior to e^+e^- annihilation, ρ_X and $\rho_{r\ old}$ are related by

$$\frac{\rho_X}{\rho_{r\ old}^{3/4}} = 0.094 rm_X. \quad (14)$$

A significant entropy increase can occur only if ρ_X begins to dominate the expansion rate at some time t_X for which $\Gamma t_X \ll 1$. The solution to Eqs. (10) - (13) for $t_X < t \ll \Gamma^{-1}$ which satisfies the boundary conditions is

$$\rho_{r\ old} = 7.9 (rm_X)^{-4/3} \left(\frac{8\pi G}{3} \right)^{-4/3} t^{-8/3}, \quad (15)$$

$$\rho_{r\ new} = \frac{4}{15} \frac{3}{8\pi G} \Gamma t^{-1}, \quad (16)$$

$$\rho_X = \frac{4}{9} \frac{3}{8\pi G} t^{-2}, \quad (17)$$

The important result here is that rm_X appears only the expression for $\rho_{r\ old}$. Define t_- to be the time at which $\rho_{r\ old} = \rho_{r\ new}$. Then Eqs. (15), (16), and (6) yield

$$\Gamma t_- = 5.1 (S_f/S_i)^{-4/5} \bar{y}_*^{-3/5} f_{e^+e^-}^{-4/5}. \quad (18)$$

For $S_f/S_i \gg 1$, $\Gamma t_- \ll 1$ and $t_X < t_-$, so the derivation of (18) is self-consistent. Now consider the evolution of H (Eq. 13). We have required ρ_X to dominate the expansion rate at $t = t_X$, and it is clear from Eqs. (15) and (17) that this implies that $\rho_X \gg \rho_{r\ old}$ for $t_X \leq t \leq t_- \ll \Gamma^{-1}$. However, for

$t > t_{\underline{=}}$, $\rho_{r\ new} \gg \rho_{r\ old}$, so $\rho_{r\ old}$ never contributes significantly to the total energy density after ρ_X begins to dominate the expansion. Consequently, the time evolution of H , the scale factor \bar{R} , and ρ_B is independent of rm_X for $t > t_X$. The time evolution of quantities which depend on ρ_r , such as T and η , will become independent of rm_X when $\rho_{r\ new} \gg \rho_{r\ old}$ which occurs for $t > t_{\underline{=}}$. From Eqs. (15) and (16),

$$t_{\underline{=}} = 11 \text{ sec } (rm_X/MeV)^{-4/5} (\tau/sec)^{3/5}. \quad (19)$$

Then for $t > t_{\underline{=}}$, the evolution of all of the parameters affecting primordial nucleosynthesis is independent of rm_X .

The earliest physical process which can affect primordial nucleosynthesis is the freeze-out of the weak reactions which keep the neutrinos in chemical equilibrium. The extent to which the photons are heated relative to the neutrinos by the decaying particles will determine the expansion rate as a function of the temperature at later times. Let t_e , t_{μ} , and t_{τ} be the times at which the electron, muon, and tau neutrinos drop out of chemical equilibrium. The electron neutrino, because of its charged current interactions with the e^+e^- pairs, stays in chemical equilibrium longer than the other neutrinos, so $t_{\mu,\tau} < t_e$. If $t_{\underline{=}} < t_{\mu,\tau}$, then all of the neutrinos freeze out after the evolution of all of the relevant parameters has become independent of rm_X . However, for $t_{\mu,\tau} < t_{\underline{=}} < t_e$, no significant heating of the μ and τ neutrinos will occur, so that $T_{\nu_{\mu}} = T_{\nu_{\tau}} \ll T_{\nu_e}$, while the evolution of T_{ν_e} and all of the other parameters affecting primordial nucleosynthesis will be independent of rm_X . The next process which affects nucleosynthesis is the freeze-out of the weak reactions which keep the neutrons and protons in equilibrium. Let t_W be the time at which these reactions freeze out. Then for $t_{\mu,\tau} < t_e < t_{\underline{=}} < t_W$, we have $T_{\nu} \ll T_{\gamma}$ for all of the neutrinos, while all of the other parameters affecting nucleosynthesis will become independent of rm_X before the $n \leftrightarrow p$ rates freeze out. This argument cannot be extended further because we have relied on the fact that the heating of the neutrinos is a discrete process; if $t_{\underline{=}} < t_{\nu}$, then the neutrino heating is independent of rm_X , while if $t_{\nu} < t_{\underline{=}} < t_W$, then $T_{\nu} \ll T_{\gamma}$ before nucleosynthesis commences. In contrast, the freeze-out of the $n \leftrightarrow p$ reactions will vary continuously with rm_X for $t_W < t_{\underline{=}}$.

To determine when the above conditions hold true, we take the the $\nu\bar{\nu}$ annihilation rates, $\Gamma_{\nu\bar{\nu}}$, to be of the form $\Gamma_{\nu\bar{\nu}} = A_{\nu} T^5$, where the constants A_{ν} , $\nu = e, \mu, \tau$, are taken to be $A_e = 0.068 \text{ sec}^{-1} \text{ MeV}^{-5}$, $A_{\mu} = A_{\tau} = 0.015 \text{ sec}^{-1} \text{ MeV}^{-5}$ (see Sec. III). The time t_{ν} , $\nu = e, \mu, \tau$, at which the neutrinos freeze out is given by the condition $\Gamma_{\nu\bar{\nu}} t_{\nu} \sim 1$. As a rough approximation, we take the rate for the $n \leftrightarrow p$ weak reactions to be $\Gamma_W \approx 1.5 \text{ sec}^{-1} \text{ MeV}^{-5} T^5$, and the time t_W at which these reactions freeze out is given by $\Gamma_W t_W \sim 1$. (The requirement that $T_W \approx 0.7 - 0.8 \text{ MeV}$ in the standard model yields $\Gamma_W \approx 3 \text{ sec}^{-1} \text{ MeV}^{-5} T^5$. However, the expression for Γ_W is used only for the case $t_{\mu,\tau} < t_e < t_{\underline{=}}$, so that $T_{\nu} \ll T_{\gamma}$, and Γ_W must be multiplied by a factor of 1/2). The temperature at $t_{\underline{=}}$ can be derived from Eqs. (15) and (16). Then we find $t_{\underline{=}} < t_{\mu,\tau}$ for

$$(rm_X/MeV) (\tau/sec)^{-7} > 1.0 \times 10^{10}, \quad (20a)$$

$t_{\mu,\tau} < t_{=} < t_e$ for

$$1.0 \times 10^{10} > (rm_X/MeV) (\tau/sec)^{-7} > 4.8 \times 10^5, \quad (20b)$$

and $t_{\mu,\tau} < t_e < t_{=} < t_W$ for

$$4.8 \times 10^5 > (rm_X/MeV) (\tau/sec)^{-7} > 1.5 \times 10^{-2}. \quad (20c)$$

When rm_X lies within one of the regions specified by Eqs. (20a) - (20c), we expect the final element abundances to depend only on η_f and τ , and to be independent of rm_X , with possible changes in the element abundances only when rm_X crosses from one region to another. The regions given by Eqs. (20a) - (20c) are demarcated by dashed lines in Fig. 1 and labelled A - C, respectively. Our derivations are valid only for $S_f/S_i \gg 1$, so these regions have been indicated only for $\epsilon \geq 2$. Our conclusions are verified by our numerical results; the element abundances become independent of rm_X for sufficiently large values of rm_X (see Figs. 2 - 8).

Although the ${}^4\text{He}$ abundance is quite sensitive to variations in all of the freeze-out processes discussed above, the amount of D and ${}^3\text{He}$ depends almost entirely on the baryon-photon ratio and the expansion rate at T_{NS} , the temperature at which the so-called deuterium bottleneck breaks ($T_{NS} \sim 0.1$ MeV, a number which varies slightly with η). These parameters determine the trace amounts of D and ${}^3\text{He}$ which are not fused into ${}^4\text{He}$. If we require $t_{=} < t(T_{NS} \sim 0.1 \text{ MeV})$, which occurs for

$$(rm_X/MeV) (\tau/sec)^{-2} > 2.1 \times 10^{-5}, \quad (20d)$$

then the expansion rate and baryon-photon ratio at T_{NS} will be independent of rm_X and will depend only on τ and η_f . When this condition is satisfied, the abundances of D and ${}^3\text{He}$ will be independent of rm_X . The region which satisfies Eq. (20d) has been labelled D in Fig. 1. Again, this conclusion is confirmed by our numerical results (Figs. 2 - 8).

III. CALCULATIONS

The computer code of Wagoner (1973) with updated reaction rates (Fowler, Caughlan, and Zimmerman 1975; Harris et al. 1983) and numerical integration of the weak rates (Dicus et al. 1982) was modified to allow for the effects of massive decaying particles. The energy density of the X particles was included in the total energy density used to determine the expansion rate (Eq. 1), where ρ_X evolves as

$$\rho_X = \rho_{X0} \left(\frac{R}{R_0} \right)^{-3} e^{-\Gamma t}. \quad (21)$$

The other important effect of the decaying X particles is the heating of the thermal background radiation. On our assumption that thermalization of the X decay products proceeds in a time much shorter than the expansion time, the time evolution of the temperature is described by

$$\frac{dT}{dt} = [-3H(\rho + p) + \Gamma_{\rho X}] / \left(\frac{d\rho}{dT}\right), \quad (22)$$

where p and ρ are the total pressure and energy density, respectively. The first term in brackets in Eq. (22) gives the standard adiabatic change in T , while the second term accounts for the heating due to the X decay.

The presence of the decaying X's will also alter the temperature at which the neutrinos freeze out and change the ratio between T_ν and T_γ . This change in T_ν alters the expansion rate and, for the electron neutrinos, it also changes the weak $n \leftrightarrow p$ rates. We have modeled this effect by assuming that the temperature for a particular neutrino tracks the photon temperature until it decouples at a time given by $\Gamma_{\nu\bar{\nu}}/H = 1$, where the $\nu\bar{\nu}$ annihilation rate, $\Gamma_{\nu\bar{\nu}}$ is taken to be of the form

$$\Gamma_{\nu\bar{\nu}} = A_\nu T^5, \quad (23)$$

and the constants A_ν , $\nu = e, \mu, \tau$, are chosen so that in the standard model, the μ and τ neutrinos decouple at $T_d = 3.5$ MeV, and the electron neutrinos decouple at $T_d = 2$ MeV (Dicus et al. 1982). After decoupling, the neutrino temperature decreases adiabatically.

Another important effect, first investigated by Lindley (1979), is the possibility that high-energy photons from the X decays might fission deuterium and other light elements. However, it will be shown (see Sec. IV) that this effect does not alter the constraints which we will place on τ and rm_X on the basis of primordial nucleosynthesis without photofission.

Wagoner's code was run over a grid in the variables τ , rm_X , and η_f . The lifetime τ was varied by factors of 10 within the range

$$10^{-2} \leq \tau \leq 10^7, \quad (24)$$

and η_f was varied by factors of $10^{0.5}$ within the constraints given by Eq. (4a). Then Eqs. (3) and (8) give an upper limit on rm_X , and the lower limit was taken to be $rm_X \geq 10^{-2}$ MeV. Within this range, rm_X was varied by factors of 10.

IV. RESULTS

Before discussing our results, it is helpful to review known limits on the various primordial element abundances. The elements of interest here are ${}^4\text{He}$, D, and ${}^3\text{He}$. Limits on the primordial abundances of these elements have been given by Yang et al. (1984) and have been reviewed most recently by Boesgaard and Steigman (1985). The abundance of ${}^4\text{He}$ is expressed as Y_p , the primordial mass fraction of ${}^4\text{He}$, while the primordial abundances of D and ${}^3\text{He}$ are expressed as their number densities relative to the number density of hydrogen, $(\text{D}/\text{H})_p$ and $({}^3\text{He}/\text{H})_p$. It is thought that astrophysical processes tend to produce ${}^4\text{He}$ and destroy D, so present observations of these elements can be used to put an upper limit on the primordial abundance of ${}^4\text{He}$ and a lower limit on the primordial abundance of D. Conservative values for these limits are (Yang et al. 1984)

$$Y_p \leq 0.25, \quad (25)$$

$$(D/H)_p \geq 1 \times 10^{-5}. \quad (26)$$

Yang et al. have also suggested that an upper limit can be placed on the sum of the primordial deuterium and helium-3 abundances $(D + {}^3\text{He}/H)_p$. This conclusion arises from the fact that deuterium in stars is burned into ${}^3\text{He}$, and an estimate can be made of the fraction of ${}^3\text{He}$ in stars which is not burned into heavier elements. Yang et al. give as a conservative upper bound

$$(D + {}^3\text{He}/H)_p \leq 1.0 \times 10^{-4}, \quad (27)$$

while their "most likely" upper limit is

$$(D + {}^3\text{He}/H)_p \leq 6.2 \times 10^{-5}. \quad (28)$$

These results are considerably more model-dependent than the limits on ${}^4\text{He}$ and D, so any conclusions based on Eqs. (27) - (28) must be treated with some skepticism (although see Dearborn, Schramm, and Steigman 1985).

The primordial abundances of ${}^4\text{He}$, D and $D + {}^3\text{He}$ are presented in Figs. 2 - 8 for the indicated values of η_f ($\eta_f = 10^{-10.5} - 10^{-7.5}$). These abundances have been interpolated within the grid described in Sec. III. The solid lines are contours of constant Y_p marked off in intervals of 0.05. The dashed lines demarcate the regions which violate the limits on (D/H) and $(D + {}^3\text{He}/H)$ given in Eqs. (26) - (28). Region A gives $(D/H)_p < 1 \times 10^{-5}$, region B yields $(D + {}^3\text{He}/H)_p > 6.2 \times 10^{-5}$, and region C gives $(D + {}^3\text{He}/H)_p > 1.0 \times 10^{-4}$. The unlettered region between dashed lines satisfies the bounds given by Eqs. (26) - (28). For $\eta_f \geq 10^{-8.5}$, $(D/H) < 10^{-5}$ for all values of τ and rm_X under consideration, while the upper limits on $(D + {}^3\text{He}/H)$ given by Eqs. (27) and (28) are satisfied everywhere for $\eta_f \geq 10^{-9}$. Values of τ , rm_X , and η_f which give $\eta_i > 10^{-4}$ are excluded; this excluded region has been indicated in Figs. 2 - 8, and no element abundances have been plotted in this region.

Several features of interest are apparent in these Figures. An increase in rm_X for fixed η_f increases both the expansion rate at early times and the initial baryon-photon ratio required to achieve this value of η_f , and both of these will tend to increase the final ${}^4\text{He}$ abundance. Although this is generally the case in Figs. 2 - 8, it was noted in Sec. II that there are large ranges in rm_X over which the element abundances become independent of rm_X . This is apparent in Figs. 2 - 8, since the curves of equal element abundance become vertical lines for large rm_X . For small values of rm_X ($rm_X \lesssim 0.3$ MeV), the presence of the X particles has no significant effect on the expansion rate during nucleosynthesis, but the element abundances will still vary with rm_X because η_i depends on rm_X for fixed η_f and τ . In the limit of large τ and small rm_X (particles which are stable throughout nucleosynthesis but not dense enough to affect the expansion rate during nucleosynthesis), we expect the element abundances to depend only on η_i . Thus, the curves of equal element abundance will also be curves of equal ϵ , parallel to those given in Fig. 1. This result is apparent in Figs. 2 - 8. For small τ and small rm_X , the decaying particles neither affect nucleosynthesis nor dilute the baryon-photon ratio, so the element abundances are the same as in the standard model with $\eta = \eta_i = \eta_f$. X particles with $\tau \leq 10^{-2}$ sec have no effect on

primordial nucleosynthesis regardless of the value of rm_X ; essentially all of the X particles decay before any processes which affect primordial nucleosynthesis begin.

We note that there are regions of anomalously low ${}^4\text{He}$ production for $\tau \sim 10^{-1}$ sec. Surprisingly, a particle with a lifetime near 10^{-1} sec actually leads to *lower* ${}^4\text{He}$ production than if there were no decaying particle present, and it gives less ${}^4\text{He}$ than a longer-lived particle with the same rm_X . The reason for this lies in the way in which the different neutrino species are heated by the X decays. For $\tau \lesssim 10^{-2}$, all three neutrino species are in thermal equilibrium during the X decays, so they are heated to the same temperature as the photons and electron-positron pairs by these decays. For $\tau \sim 10^{-1}$ sec, the neutrinos drop out of equilibrium at about the same time that most of the heating from the X decays is occurring. The electron neutrino, because of its charged current reactions with the e^+e^- pairs, interacts more strongly than the muon and tau neutrinos, so it stays in equilibrium longer with the $e^\pm\gamma$ plasma, resulting in $T_{\nu_e} \approx T_\gamma$, while the other two neutrino species decouple before all the X's decay, so that $T_{\nu_\mu} = T_{\nu_\tau} < T_\gamma$. The amount of ${}^4\text{He}$ produced is most dependent on the temperature at which the weak $n \leftrightarrow p$ reactions freeze out. This freeze-out temperature is a function of the weak rates, which depend on the photon and electron neutrino temperatures, and of the expansion rate, which depends on the photon temperature and all of the neutrino temperatures. For a decaying particle with a lifetime $\sim 10^{-1}$ sec, the electron neutrinos are heated to roughly the same temperature relative to the photon temperature as in the standard model, but the other neutrinos have a much lower temperature than they do in the standard model when the $n \leftrightarrow p$ reactions freeze out. The net result is that the weak rates at a given photon temperature are unaltered, while the total energy density and, therefore, the expansion rate at this temperature are lower than in the standard model: $\rho(T) = \rho_\gamma(T) + \rho_{e^+e^-}(T) + \rho_{\nu_e}(T) + \rho_{\nu_\mu}(T') + \rho_{\nu_\tau}(T')$, with $T' < T$. This allows the $n \leftrightarrow p$ reactions to freeze out at a lower temperature, resulting in less ${}^4\text{He}$. For still larger values of the X lifetime, the electron neutrinos are also unheated by the X decays, reducing the $n \leftrightarrow p$ rates as a function of T_γ , while for sufficiently large τ , the X particles begin to dominate the expansion rate when the $n \leftrightarrow p$ reactions freeze out. Both of these effects result in a higher freeze-out temperature and more ${}^4\text{He}$ as τ is increased. When τ is much larger than the nucleosynthesis time scale (~ 100 sec), the only dependence of the ${}^4\text{He}$ abundance on τ arises from the fact that η_i depends on τ for fixed η_f . The ${}^4\text{He}$ abundance, however, is relatively insensitive to the value of η_i for large η_i ; essentially all of the neutrons left over from the freeze-out of the $n \leftrightarrow p$ reactions are burned into ${}^4\text{He}$. Thus, for large values of rm_X and τ , the ${}^4\text{He}$ abundance is relatively independent of τ .

In the standard model, the abundance of deuterium is highly sensitive to the baryon-photon ratio, and this remains true in models with decaying particles. If we require $(\text{D}/\text{H})_p \geq 10^{-5}$, then we must have $\eta_f \leq 10^{-9}$ regardless of the presence of decaying particles. (Although our results indicate only a small allowed region for $(\text{D}/\text{H})_p \geq 10^{-5}$ and $\eta_f = 10^{-9}$, the actual value of (D/H) is only very slightly less than 10^{-5} over much of the τ, rm_X plane for this value of η_f). If we

further require $(D + {}^3\text{He}/\text{H}) \leq 1.0 \times 10^{-4}$ or 6.2×10^{-5} , then the allowed region in the τ , rm_X plane becomes very narrow for $\eta_f \leq 10^{-10}$. However, the primordial ${}^4\text{He}$ abundance is relatively less sensitive to the value of η_f . For $Y_p \leq 0.25$, it is possible to choose τ and rm_X so that η_f can be as large as 10^{-8} ; a value of η_f this large requires $\tau \sim 10^{-1}$ sec. In the standard model, this upper bound on Y constrains η to be $\leq 7 \times 10^{-10}$ (Yang et al. 1984). Combining the limits on $(D/\text{H})_p$, $(D + {}^3\text{He}/\text{H})_p$, and Y_p , we find no allowed regions in the τ , rm_X plane for $\eta_f \geq 10^{-9}$, while allowed regions exist for $\eta_f \leq 10^{-9.5}$. This is to be expected, because for sufficiently low values of rm_X , the only effect of the decaying particles is to dilute the baryon-photon ratio. We can take η_i to give the correct element abundances in the standard model ($3-4 \times 10^{-10} < \eta_i < 7-10 \times 10^{-10}$) (Yang et al. 1984) and then choose τ and rm_X to give any lower value of η_f without altering the final element abundances.

Our results can also be used to rule out values of the lifetime and density parameter for any decaying particle, independent of the value of η_f . The requirement that $\eta_i \leq 10^{-4}$ and $\eta_f \geq 10^{-10.5}$ gives a constraint on τ and rm_X via Eqs. (6) and (8). This excluded region is marked as region A in Fig. 9. The constraint on primordial ${}^4\text{He}$ production ($Y_p \leq 0.25$) yields different excluded regions for different values of η_f ; however, we find that for all values of τ and rm_X , ${}^4\text{He}$ production increases with η_f , so any values of τ and rm_X which overproduce ${}^4\text{He}$ for the smallest allowed value of η_f will also produce too much ${}^4\text{He}$ for all other allowed values of η_f . Thus, the region which yields $Y_p > 0.25$ for $\eta_f = 10^{-10.5}$ can be ruled out for all η_f ; this region has been designated region B in Fig. 9. Regions A and B together give a safe upper limit on τ and rm_X ; for large values of rm_X ($\geq 10^4$ MeV) we find $\tau \leq 10$ sec.

Less secure limits can be placed on τ and rm_X from the upper bounds on $(D + {}^3\text{He}/\text{H})_p$. We find that $(D + {}^3\text{He}/\text{H})_p$ decreases as η_f increases for all τ and rm_X , so that any region which is excluded for the largest possible value of η_f will be excluded for all η_f . Unfortunately, it turns out that for $\eta_f \geq 10^{-9}$, the upper bounds on $(D + {}^3\text{He}/\text{H})_p$ are satisfied for all values of τ and rm_X , so this sort of argument is useless here. However, a somewhat more complicated but still rigorous argument can be used. Note that for any fixed τ and rm_X , the ${}^4\text{He}$ abundance increases and the $(D + {}^3\text{He}/\text{H})$ value decreases as η_f is increased. Then for any value of η_f , a choice of τ and rm_X which overproduces both ${}^4\text{He}$ and $D + {}^3\text{He}$ can be ruled out for all values of η_f ; increasing η_f will still yield too much ${}^4\text{He}$, while decreasing η_f will continue to produce too large a value of $(D + {}^3\text{He}/\text{H})$. Thus, we can go through each of our values for η_f and exclude all regions which overproduce both ${}^4\text{He}$ and $D + {}^3\text{He}$. These regions have been designated C and D in Fig. 9. Region C is derived from Fig. 3 ($\eta_f = 10^{-10}$) and our more conservative limit on $(D + {}^3\text{He}/\text{H})$ (Eq. 27), while region D comes from the less conservative limit (Eq. 28) and Figs. 3 and 4 ($\eta_f = 10^{-10} - 10^{-9.5}$). Our most restrictive but least certain bound on τ for large values of rm_X is $\tau \leq 1$ sec for $rm_X \geq 400$ MeV.

Finally, we note that the region in the τ , rm_X plane which can be excluded because it requires $\eta_i > 10^{-4}$ behaves in the same way as the region which can be

excluded on the basis of ${}^4\text{He}$ production, i.e., the excluded region which gives $\eta_i > 10^{-4}$ becomes larger as η_f increases. Therefore, for each value of η_f , we can rule out regions which require $\eta_i > 10^{-4}$ and overproduce $\text{D} + {}^3\text{He}$ by an argument similar to that used above. Region E in Fig. 9 gives the area which yields $\eta_i > 10^{-4}$ and $(\text{D} + {}^3\text{He}/\text{H})_p > 1.0 \times 10^{-4}$ for $\eta_f = 10^{-10}$, while region F gives $\eta_i > 10^{-4}$ and $(\text{D} + {}^3\text{He}/\text{H})_p > 6.2 \times 10^{-5}$ for $\eta_f = 10^{-9.5}$.

There is some overlap between the various excluded regions of Fig. 9; this overlap has been suppressed. Some of the excluded regions have a rather irregular shape, which is due to the fact that we are forced to use discrete values of η_f in deriving these regions. If we were able to vary η_f continuously, and then excluded any values of τ and rm_X which yielded the wrong element abundances for all values of η_f , then we would expect the boundaries of the excluded regions to be less irregular in shape. However, in determining our excluded regions, we have erred on the side of caution. All of the excluded regions in Fig. 9 would still be excluded if we had used smaller increments in η_f ; the only effect of varying η_f more continuously would be to enlarge the excluded region slightly.

An effect which we have not included in our simulations is the destruction of the primordial light elements by photofission due to high-energy photons from the X decays (Lindley 1979; for more recent discussions, see Lindley 1980, 1985; Scherrer 1984; Ellis, Nanopoulos, and Sarkar 1985). This effect will be important for X lifetimes which allow significant X decay to occur after the end of primordial nucleosynthesis; photofission which terminates before nucleosynthesis begins will be irrelevant because the deuterium will simply readjust to its equilibrium abundance after photofission ends, and there are no other light nuclei present (except, of course, hydrogen) before nucleosynthesis begins. One might think that it would be possible to induce photofission for arbitrarily short lifetimes by increasing the X energy density, but this turns out to be self-defeating. At sufficiently early times, the dominant thermalization mechanism for the decay photons is $\gamma\gamma \rightarrow e^+e^-$, the decay photon reacting with a background photon. However, for $t \gtrsim \tau$, the photon dilution factor is proportional to rm_X . The photofission rate for all of the nuclei is essentially proportional to the X energy density and inversely proportional to the thermalization rate for the decay photons. Then the photofission rate for large rm_X and $t \gtrsim \tau$ contains two factors of rm_X which cancel each other, and the photofission rate is independent of rm_X . This is essentially the same argument as that used in Sec. II. The requirement that photofission occur after nucleosynthesis indicates that photofission will have no effect on the final element abundances for $\tau \lesssim 10^2$ sec.

More importantly, photofission cannot alter the final element abundances in such a way as to cause any of the excluded regions in Fig. 9 to become allowed. For most choices of the decaying particle mass, lifetime, and abundance, the photofission rate per ${}^4\text{He}$ nucleus is roughly comparable to the photofission rates for D and ${}^3\text{He}$, while the abundance of ${}^4\text{He}$ after nucleosynthesis is $\gtrsim 10^4$ times larger than the D and ${}^3\text{He}$ abundances. Thus, the effect of photofission under most circumstances is to increase, rather than decrease the D and ${}^3\text{He}$ abundances (Ellis, Nanopoulos, and Sarkar 1985). If the ${}^4\text{He}$ abundance is too large, it may be possible to reduce this abundance to an acceptable level through fission of

the ${}^4\text{He}$, but the D and ${}^3\text{He}$ produced by this fission will be far more abundant than the accepted upper bounds. The only way to reduce the D and ${}^3\text{He}$ abundances through photofission is to destroy essentially all of the ${}^4\text{He}$, leaving only trace amounts of ${}^4\text{He}$, ${}^3\text{He}$, and D. However, the observed ${}^4\text{He}$ must then be produced non-primordially. Thus, the regions in Fig. 9 which we have ruled out because they overproduce ${}^4\text{He}$ or D + ${}^3\text{He}$ will continue to be ruled out after photofission is taken into account. A bound which can be circumvented via photofission is the requirement that $(\text{D}/\text{H})_p \geq 10^{-5}$. It is possible to produce small amounts of D and ${}^3\text{He}$ by means of photofission without significantly altering the ${}^4\text{He}$ abundance, although the production of the correct amount of D and ${}^3\text{He}$ requires a delicate fine-tuning of the decaying particle lifetime (see Audouze, Lindley, and Silk 1985). However, we have not used this bound on $(\text{D}/\text{H})_p$ in determining the excluded regions of Fig. 9. A caveat must be added to these remarks: there are some circumstances under which the photofission rate for ${}^4\text{He}$ can be much larger than the deuterium photofission rate. The threshold for ${}^4\text{He}$ fission is ≈ 20 MeV, while the photofission threshold for deuterium is 2.225 MeV. If the X particle mass were such that the decay photons had energies between 2 and 20 MeV, then only deuterium fission would occur. Furthermore, photon thermalization proceeds very efficiently via $\gamma\gamma \rightarrow e^+e^-$ when $E_\gamma T \gtrsim m_e^2$. If the decay occurs at a temperature when 20 MeV photons can thermalize via this reaction, but 2 MeV photons cannot, then the photofission rate for D will be much larger than for ${}^4\text{He}$.

We now give three examples of how to apply our results to actual particles. Consider first the case of a massive, fourth-generation neutrino, ν_H , with only the standard electroweak interaction of the Weinberg-Salam-Glashow theory. For $m_{\nu_H} \gtrsim 2m_e$, the dominant decay mode will be $\nu_H \rightarrow \nu_L e^+ e^-$, where ν_L is the neutrino mass eigenstate which couples most strongly to the electron. This decay mode converts roughly 2/3 of the neutrino mass into electromagnetic entropy, so our results for total conversion of the decaying particle mass into electromagnetic entropy represent a reasonable approximation. If $m_{\nu_H} \gg m_{\nu_L}$, then the neutrino lifetime can be scaled from the muon lifetime:

$$\tau_{\nu_H} = \tau_\mu (m_{\nu_H}/m_\mu)^{-5} 4 \sin^{-2} 2\theta, \quad (29)$$

where θ is the mixing angle between the ν_H and ν_L mass eigenstates and the electron-type weak interaction eigenstate. Mixing of any other neutrino mass eigenstates with the electron has been ignored. A derivation of τ for the massive neutrino requires an integration of the rate equations governing the neutrino abundance in the early universe (although see Scherrer and Turner 1985b). Such an integration has been performed by Kolb and Scherrer (1982). Their results are given in terms of Y_ν , the number density of a single neutrino spin state divided by the photon number density after e^+e^- annihilation. Thus, $rm_X = (Y_\nu)(2)(11/4)(m_{\nu_H})$. For $m_{\nu_H} \sim 10 - 100$ MeV, Y_ν is well-approximated (within 10 %) by $Y_\nu = 3.8 (m_{\nu_H}/\text{MeV})^{-2.5}$, so

$$rm_X = (21 \text{ MeV}) (m_{\nu_H}/\text{MeV})^{-1.5}. \quad (30)$$

We have used Eq. (29) and the numerical results for rm_X to plot the τ , rm_X

values for the massive neutrino in Fig. 10. Each curve corresponds to the indicated value of the mixing angle θ , and these curves have been superimposed over the line from Fig. 9 demarcating the forbidden region in the τ , rm_X plane. We can then rule out $m_{\nu_B} \sim 3 - 20$ MeV ($\sin \theta = 10^{-3}, 10^{-4}$), $m_{\nu_B} \sim 3 - 10$ MeV ($\sin \theta = 10^{-2}$), and $m_{\nu_B} \sim 3 - 4$ MeV ($\sin \theta = 0.2$), where the lower bound has been set at 3 MeV to satisfy the constraint that $m_{\nu_B} \gg m_e$.

Now consider the case of the gravitino, the supersymmetric partner of the graviton. Weinberg (1982) was the first to consider the effect of decaying gravitinos on primordial nucleosynthesis, although he assumed that the gravitino decays merely heated up the black-body temperature, allowing the Universe to go through nucleosynthesis again. Since such reheating does not occur, we give a revised version of Weinberg's calculation. Weinberg assumed that the gravitino drops out of thermal equilibrium near the Planck time, when it is still relativistic. Then the abundance of gravitinos relative to photons at T_0 is given by

$$r = \frac{3}{4} [g_\lambda(T_0)/g_\lambda(T_e)], \quad (31)$$

where T_e is the temperature at which the gravitinos drop out of equilibrium, and $g_\lambda(T_0) = 43/4$. We have taken $r = 10^{-2}$, corresponding to $g_\lambda(T_e) \sim 10^3$. Then

$$rm_X = 10^{-2} m_{3/2}, \quad (32)$$

where $m_{3/2}$ is the gravitino mass, and we take

$$\tau = 10^8 \text{ sec } (m_{3/2}/100 \text{ GeV})^{-3}. \quad (33)$$

The values of τ and rm_X from Eqs. (32) - (33) are displayed in Fig. (10). The allowed gravitino mass is $m_{3/2} \gtrsim 10^5$ GeV, relatively independent of r ; this bound is valid for $r \sim 10^{-5} - 10^{-2}$. By assuming that the gravitino decay heated up the radiation background, Weinberg (1982) derived the limit $m_{3/2} \gtrsim \xi^{-1/3} \times 10^4$ GeV, where ξ is a dimensionless parameter $\lesssim 1$. Thus, our bound is an order of magnitude more stringent than Weinberg's.

In inflationary Universe models, any primordial abundance of gravitinos is exponentially diluted, and any gravitino production takes place during reheating following inflation; the post-reheating gravitino abundance relative to photons is given by (Ellis, Kim, and Nanopoulos 1984; also see Krauss 1983)

$$n_{3/2}/n_\gamma = 1.38 \times 10^{-11} T_{\theta R} (1 - 0.018 \ln T_{\theta R}), \quad (34)$$

where $T_{\theta R}$ is the maximum reheating temperature in units of 10^9 GeV. Using the constancy of the entropy per comoving volume, $R^3 g_* T_\gamma^3$, the gravitino to photon ratio at $T_0 \sim 10^{12}$ K is

$$r = 1.38 \times 10^{-11} [g_\lambda(T_0)/g_\lambda(T_R)] T_{\theta R} (1 - 0.018 \ln T_{\theta R}). \quad (35)$$

In the minimal supersymmetric standard model, $g_\lambda(T_R) = 915/4$ (Ellis, Kim, and Nanopoulos 1984), while $g_\lambda(T_0) = 43/4$. Then

$$rm_X = 6.46 \times 10^{-13} m_{3/2} T_{\theta R} (1 - 0.018 \ln T_{\theta R}). \quad (36)$$

The value of the gravitino lifetime depends on the particular decay channels

which are open. For gravitino decay into $\tilde{\gamma}\tilde{\gamma}$, the lifetime is (Ellis, Kim, and Nanopoulos 1984)

$$\tau = 4 \times 10^8 \text{ sec } (m_{3/2}/100 \text{ GeV})^{-3}, \quad (37)$$

while if the $g\tilde{g}$ channel is also open,

$$\tau = 4.4 \times 10^7 \text{ sec } (m_{3/2}/100 \text{ GeV})^{-3}. \quad (38)$$

The fraction of the gravitino mass converted into electromagnetic entropy is roughly 1/2 for decay into $\tilde{\gamma}\tilde{\gamma}$ and 4/5 if decay into $g\tilde{g}$ is also allowed (Ellis, Kim, and Nanopoulos 1984). Thus, it is again a reasonable approximation to use our results for total conversion into electromagnetic entropy. As an example, we take $T_R = 10^{15}$ GeV and allow τ to vary between the values given by Eqs. (37) and (38). Then the values for τ and rm_X given by Eqs. (34) - (36) are shown in Fig. (10) for $m_{3/2} = 10^3 - 10^5$ GeV. For this value of T_R , we can exclude $m_{3/2} \lesssim 10^4$ GeV, but it is clear that a slightly lower reheating temperature prevents us from excluding any values for the mass of a gravitino with a lifetime $\lesssim 10^7$ sec. A case of particular interest is $m_{3/2} \approx m_W \approx 100$ GeV. For this value of the gravitino mass, our limit on the reheating temperature is $T_R \lesssim 10^{14}$ GeV; in this case, photofission yields a much more stringent bound (Ellis, Nanopoulos, and Sarkar 1985).

V. CONCLUSIONS

A massive, decaying particle affects primordial nucleosynthesis by increasing the expansion rate, altering the time-temperature relationship, and diluting the baryon-photon ratio. However, the decaying particle does not cause the Universe to "reheat" (Scherrer and Turner 1985a), so the Universe only goes through nucleosynthesis once. Fixing the final baryon-photon ratio η_f , we find that the ${}^4\text{He}$ abundance produced in models with massive, decaying particles is larger than in the standard model with the same value of η , and the ${}^4\text{He}$ abundance increases with increasing massive particle lifetime τ and density parameter rm_X ($r \equiv n_X/n_\gamma$ at $T = 10^{12}$ K). An exception to this arises for a decaying particle lifetime $\sim 10^{-1}$ sec, for which the ${}^4\text{He}$ abundance decreases below the amount produced in the standard model. From the upper bound on ${}^4\text{He}$ production, $Y_p \leq 0.25$, the presence of decaying particles allows η_f as large as 10^{-8} , although the possibility of η_f near this upper bound requires a decaying particle with $\tau \sim 10^{-1}$ sec. The deuterium abundance remains highly sensitive to the baryon-photon ratio when decaying particles are introduced, and the requirement that sufficient D be produced, $(\text{D}/\text{H})_p \geq 10^{-5}$, gives an upper limit on the final baryon-photon ratio of $\eta_f \leq 10^{-9}$, independent of any of the decaying particle parameters. It is possible to rule out values of the decaying particle lifetime and density parameter independent of the baryon-photon ratio; we have summarized this in Fig. 9. For large values of the density parameter ($rm_X \gtrsim 400 - 10^4$ MeV), the decaying particle lifetime must be $\lesssim 1 - 10$ sec, depending on which element abundance bounds are used. (All of the primordial element abundances become independent of rm_X for sufficiently large values of rm_X). These limits are unaffected by any photofission of the light elements from the decay photons. Although in some

cases more stringent bounds than ours can be placed on rm_X from considerations of photofission (e.g., for the gravitino, see Ellis, Nanopoulos, and Sarkar 1985; also Khlopov and Linde 1984), our results give the most stringent bounds on particles with lifetimes $\lesssim 100$ sec. More detailed plots of the element abundances and a discussion of ${}^7\text{Li}$ production will be given elsewhere.

We thank Robert Wagoner for providing us with his nucleosynthesis code, and John Conway for assistance with the Fermilab Cyber computers. This work was supported in part by the DOE (contract AC02-80ER-10773 at Chicago and Fermilab), the NASA (at Fermilab), by R.J. Scherrer's McCormick Fellowship, and by M.S. Turner's Alfred P. Sloan Fellowship.

References

- Audouze, J., Lindley, D., and Silk, J. 1985, *Ap.J. (Letters)*, 293, L53.
- Boesgaard, A. M., and Steigman, G. 1985, *Ann. Rev. Astr. Ap.*, in press.
- Bopp et al. 1984, *J. de Phys. (Colloq.)*, 45, 21.
- Dearborn, D. S. P., Schramm, D. N., and Steigman, G. 1985, *Ap.J.*, in press.
- Dicus, D. A., Kolb, E. W., Gleeson, A. M., Sudarshan, E. C. G., Teplitz, V. L., and Turner, M. S. 1982, *Phys. Rev. D*26, 2694.
- Dicus, D. A., Kolb, E. W., and Teplitz, V. L. 1978, *Ap.J.*, 221, 327.
- Ellis, J., Kim, J. E., and Nanopoulos, D. V. 1984, *Phys. Lett. B*, 145, 181.
- Ellis, J., Nanopoulos, D. V., and Sarkar, S. 1985, *Nucl. Phys. B*, 259, 175.
- Faber, S. M., and Gallagher, J. S. 1979, *Ann. Rev. Astr. Ap.*, 17, 135.
- Fowler, W. A., Caughlan, G. R., and Zimmerman, B. A. 1975, *Ann. Rev. Astr. Ap.*, 13, 69.
- Freese, K., and Schramm, D. N. 1984, *Nucl. Phys. B*, 233, 167.
- Gunn, J. E., Lee, B. W., Lerche, I., Schramm, D. N., and Steigman, G. 1978, *Ap.J.*, 223, 1015.
- Harris, M. J., Fowler, W. A., Caughlan, G. R., and Zimmerman, B. A. 1983, *Ann. Rev. Astr. Ap.*, 21, 165.
- Khlopov, M. Yu., and Linde, A. D. 1984, *Phys. Lett. B*, 138, 265.
- Kolb, E. W., and Scherrer, R. J. 1982, *Phys. Rev. D*25, 1481.
- Kolb, E. W., and Turner, M. S. 1983, *Ann. Rev. Nucl. Part. Sci.*, 33, 645.
- Kolb, E. W., Turner, M. S., and Walker, T. 1985, preprint.
- Krauss, L. L. 1983, *Nucl. Phys. B*, 227, 556.
- Lindley, D. 1979, *M.N.R.A.S.*, 188, 15P.
- _____. 1980, *M.N.R.A.S.*, 193, 593.
- _____. 1985, *Ap. J.*, 294, 1.
- Olive, K. A., Schramm, D. N., and Steigman, G. 1981, *Nucl. Phys. B*, 180, 497.
- Olive, K. A., Schramm, D. N., Steigman, G., Turner, M. S., and Yang, J. 1981, *Ap. J.*, 246, 557.
- Scherrer, R. J. 1984, *M.N.R.A.S.*, 210, 359.
- Scherrer, R. J., and Turner, M. S. 1985a, *Phys. Rev. D*31, 681.
- _____. 1985b, *Phys. Rev. D*, submitted.
- _____. 1985c, in preparation.
- Shvartsman, V. F. 1969, *JETP Lett.*, 9, 184.
- Steigman, G. 1979, *Ann. Rev. Nucl. Part. Sci.*, 29, 313.

- Steigman, G., Olive, K. A., and Schramm, D. N. 1979, Phys. Rev. Letters, 43, 239.
- Steigman, G., Schramm, D. N., and Gunn, J. E. 1977, Phys. Lett. B, 66, 202.
- Steigman, G., and Turner, M. S. 1985, Nucl. Phys. B, 253, 375.
- Szalay, A. S. 1981, Phys. Lett. B, 101, 453.
- Wagoner, R. V. 1973, Ap. J., 179, 343.
- Weinberg, S. 1982, Phys. Rev. Letters, 48, 1303.
- Wohl, C. G. et al. 1984, Rev. Mod. Phys., 56, S1.
- Wolfram, S. 1979, Phys. Lett. B, 82, 65.
- Yang, J., Schramm, D. N., Steigman, G., and Rood, R. T. 1979, Ap. J. 227, 697.
- Yang, J., Turner, M. S., Steigman, G., Schramm, D. N., and Olive, K. A. 1984, Ap. J., 281, 493.

Figure Captions

Figure 1: Solid lines give the entropy dilution factor $\epsilon \equiv \eta/\eta'$ for a decaying particle with a lifetime τ and a density parameter rm_X , where m_X is the particle mass and r is the number density of the particles relative to photons at $T \sim 10^{12}$ K; η' is the final baryon-photon ratio after the particle has decayed, and η is the final baryon-photon ratio without the decaying particles. Horizontal dashed line denotes minimum rm_X value (~ 0.3 MeV) necessary to significantly affect the expansion rate during nucleosynthesis (cf. Eq. 2). Lettered dashed lines demarcate rm_X regions for which final element abundances are independent of rm_X (see Sec. II).

Figure 2: Primordial abundances of ${}^4\text{He}$, D, and $\text{D} + {}^3\text{He}$ produced in the presence of a decaying particle as a function of the particle lifetime τ and density parameter rm_X , where m_X is the particle mass and r is the number density of the particles relative to photons at $T \sim 10^{12}$ K. Solid lines are contours of constant Y_p (primordial ${}^4\text{He}$ mass fraction) in intervals of 0.05. Dashed lines demarcate regions which underproduce deuterium or overproduce $\text{D} + {}^3\text{He}$: region A underproduces deuterium; regions B - C overproduce $\text{D} + {}^3\text{He}$. The solid line across the upper right-hand corner gives the region with an initial baryon-photon ratio larger than can be produced in the standard models for baryogenesis. This figure is for a baryon-photon ratio today of $\eta_f = 10^{-10.5}$.

Figure 3: As Fig. 2, for a baryon-photon ratio today of $\eta_f = 10^{-10}$.

Figure 4: As Fig. 2, for a baryon-photon ratio today of $\eta_f = 10^{-9.5}$.

Figure 5: As Fig. 2, for a baryon-photon ratio today of $\eta_f = 10^{-9}$.

Figure 6: As Fig. 2, for a baryon-photon ratio today of $\eta_f = 10^{-8.5}$.

Figure 7: As Fig. 2, for a baryon-photon ratio today of $\eta_f = 10^{-8}$.

Figure 8: As Fig. 2, for a baryon-photon ratio today of $\eta_f = 10^{-7.5}$.

Figure 9: Excluded values of a decaying particle lifetime τ and density parameter rm_X , where m_X is the particle mass and r is the number density of the particles relative to photons at $T \sim 10^{12}$ K. Region A violates bounds on the dilution of the baryon-photon ratio. Region B overproduces ${}^4\text{He}$. Regions C - D are derived from combinations of bounds on the ${}^4\text{He}$ and $\text{D} + {}^3\text{He}$ abundances, and regions E - F are from bounds on the $\text{D} + {}^3\text{He}$ abundance and limits on the production of entropy. All bounds are independent of the present baryon-photon ratio, subject only to the assumption that η today is $\geq 3 \times 10^{-11}$.

Figure 10: Values of τ and rm_X for a fourth-generation massive neutrino and two scenarios for gravitino production. Solid lines near the bottom give τ , rm_X values for a massive neutrino with indicated values of the mixing angle. Horizontal segments give τ , rm_X values for a gravitino with the indicated masses regenerated after inflation, assuming a reheating temperature of 10^{15} GeV. Solid line near the top gives τ , rm_X values for primordial gravitinos which had an abundance comparable to the photon abundance at the Planck time. Heavy line demarcates the forbidden region in the τ , rm_X plane.

FIG. 1

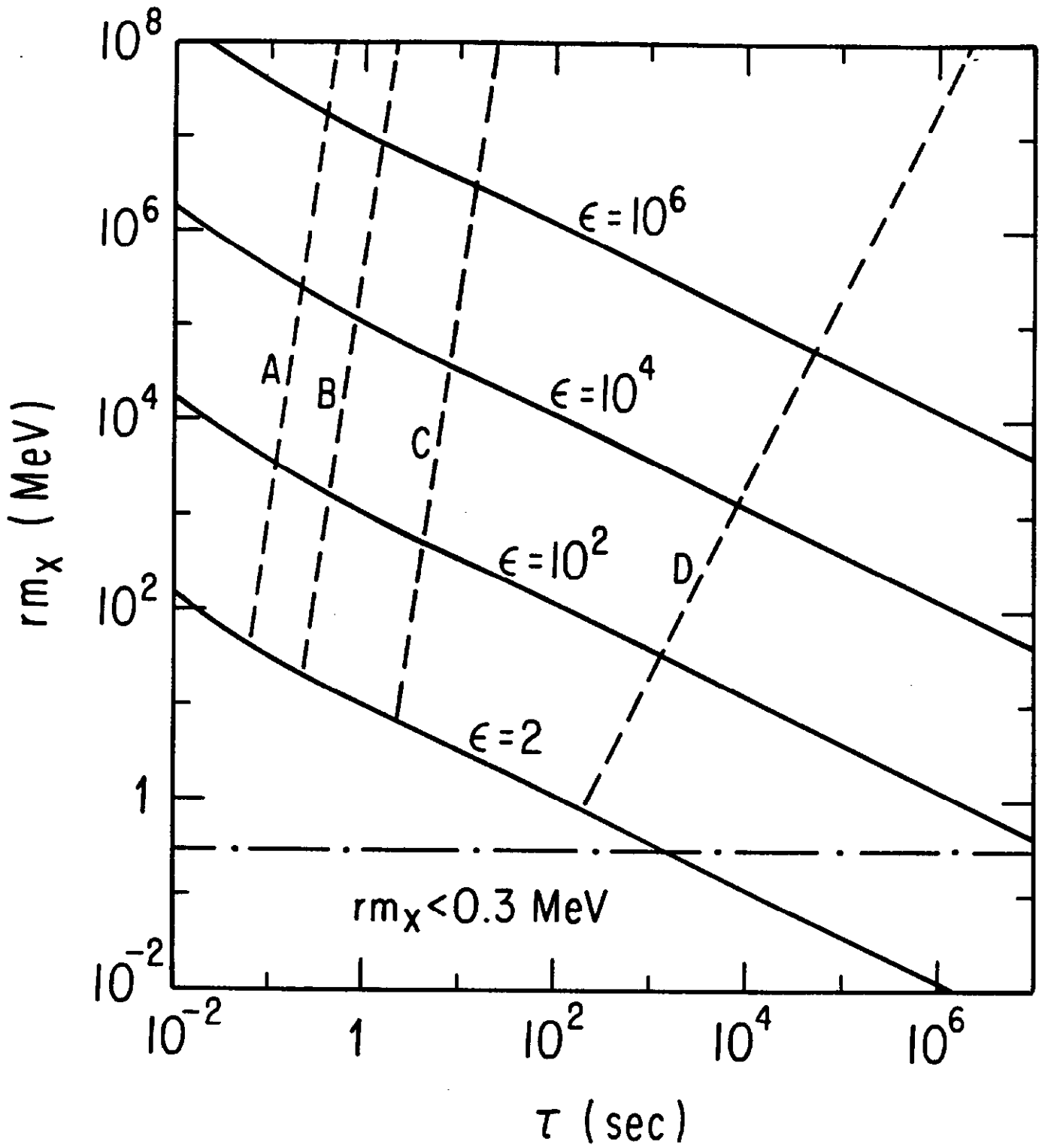


FIG. 2

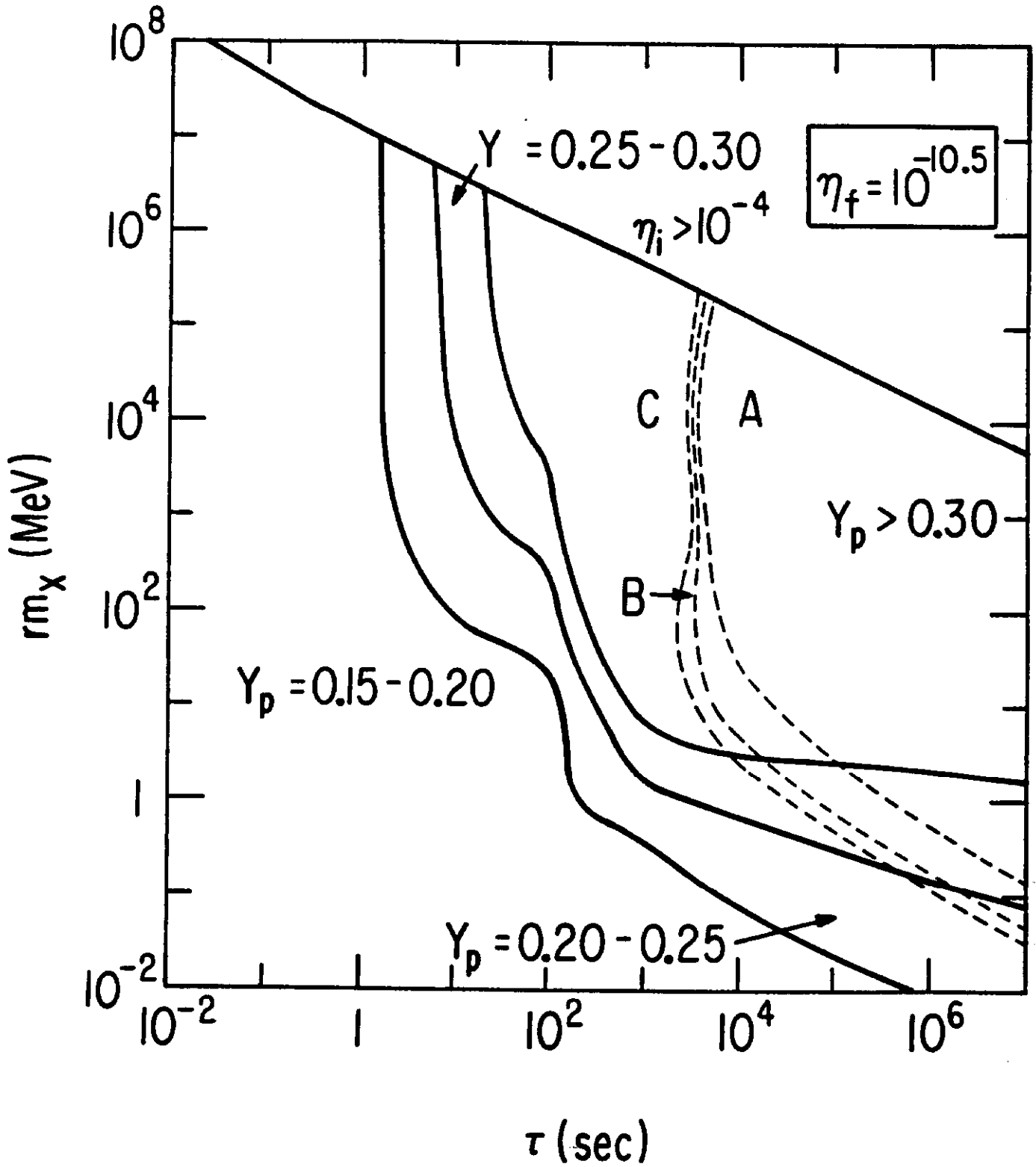


FIG. 3

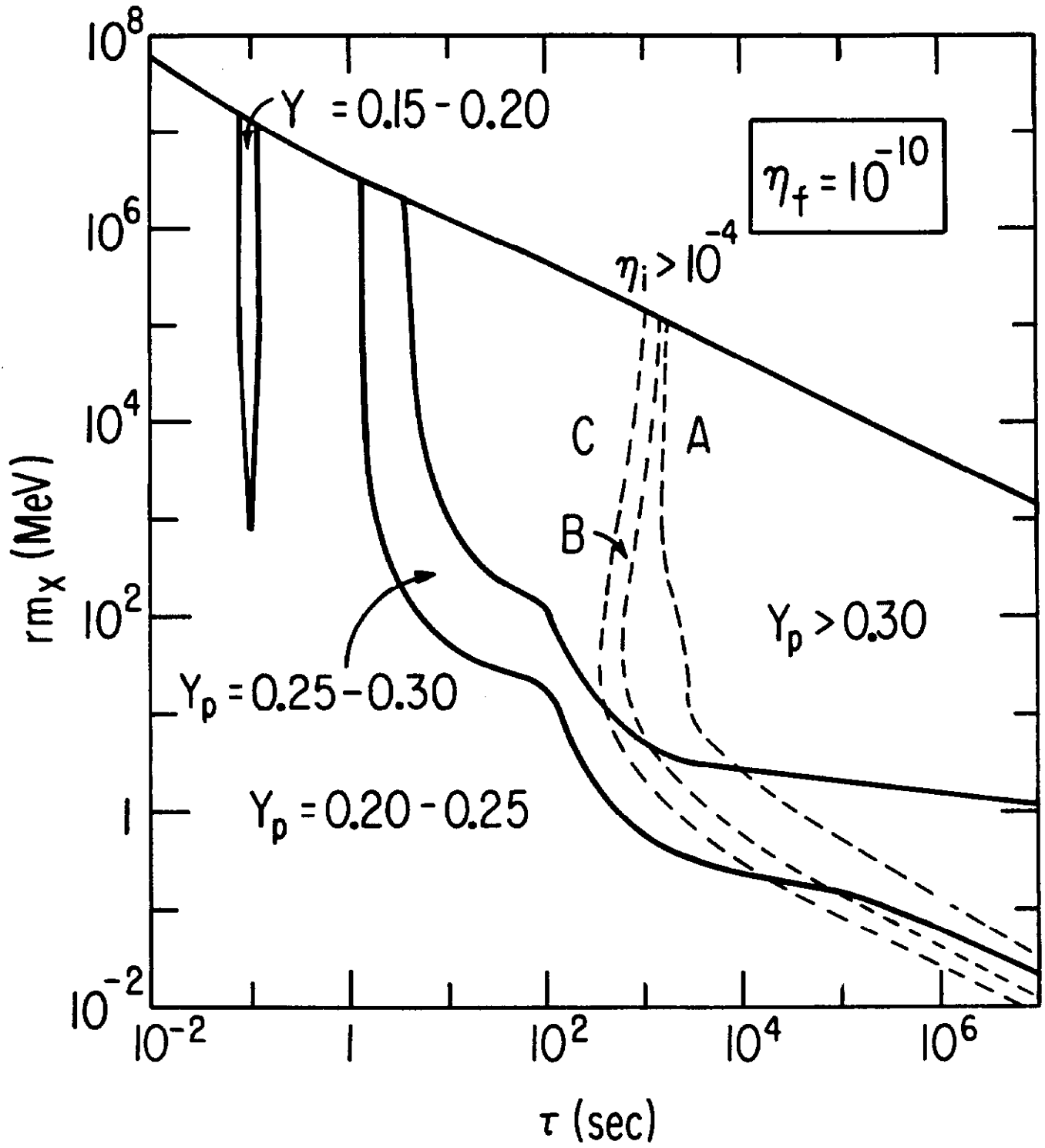


FIG. 4

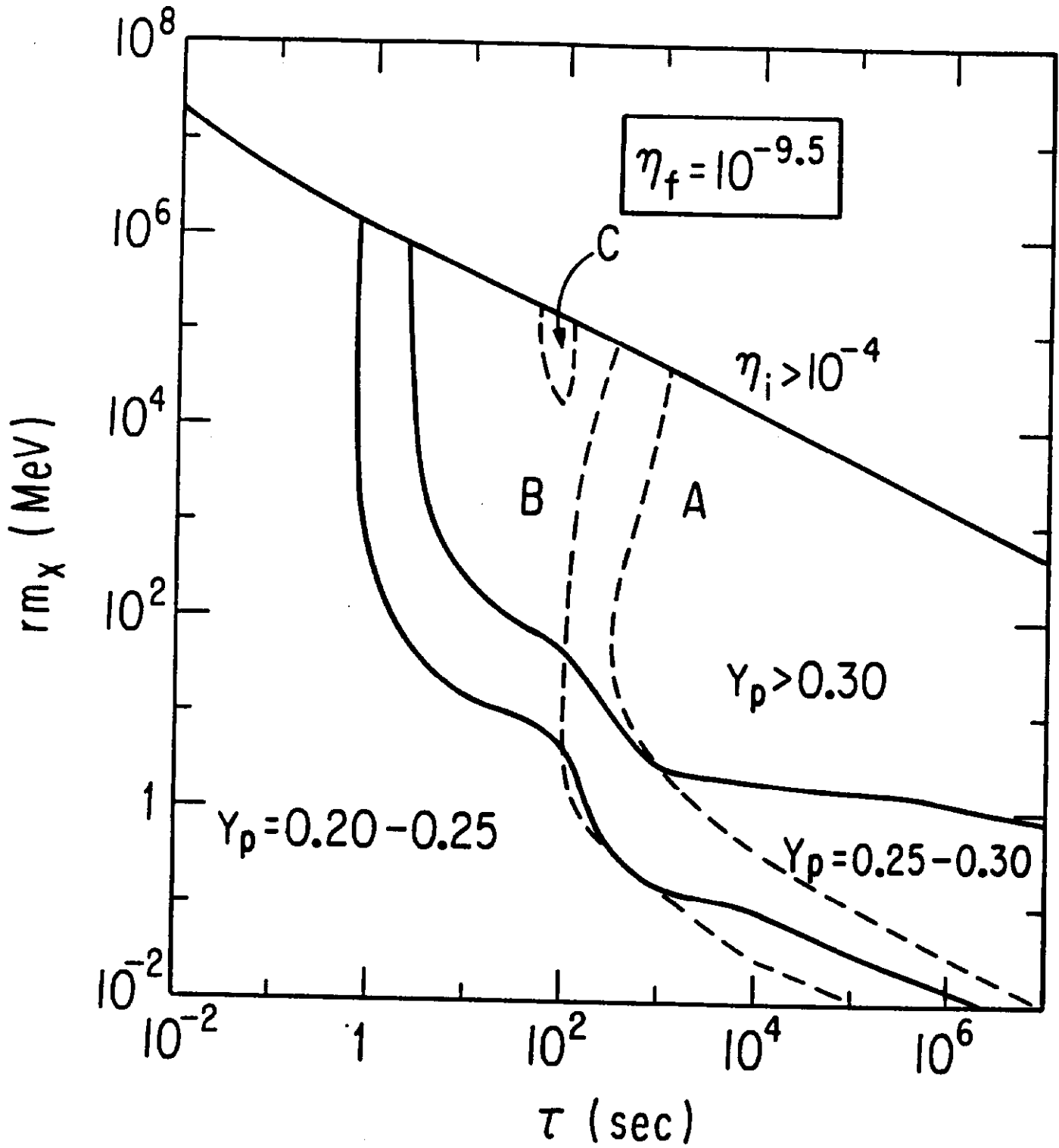


FIG. 5

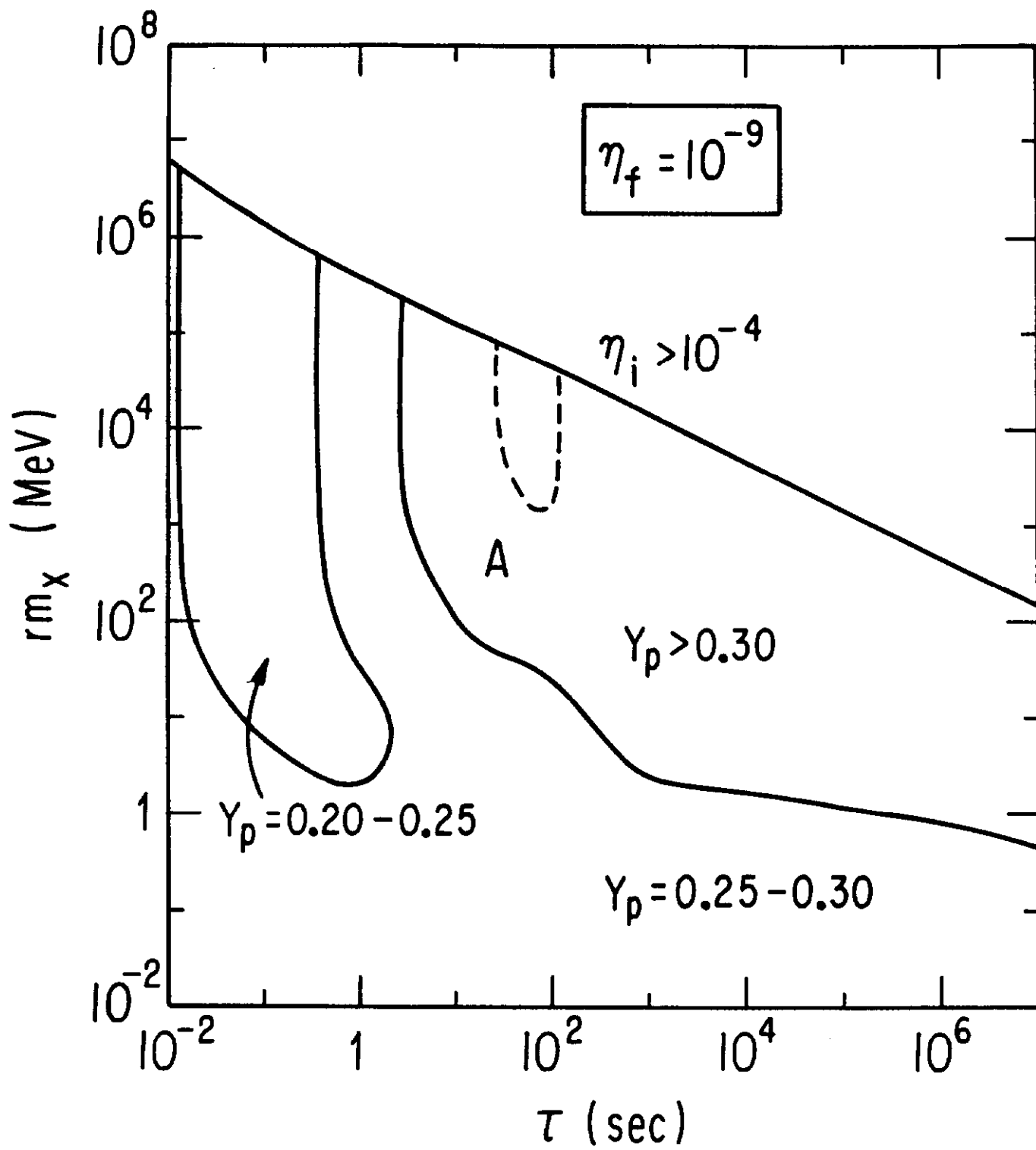


FIG. 6

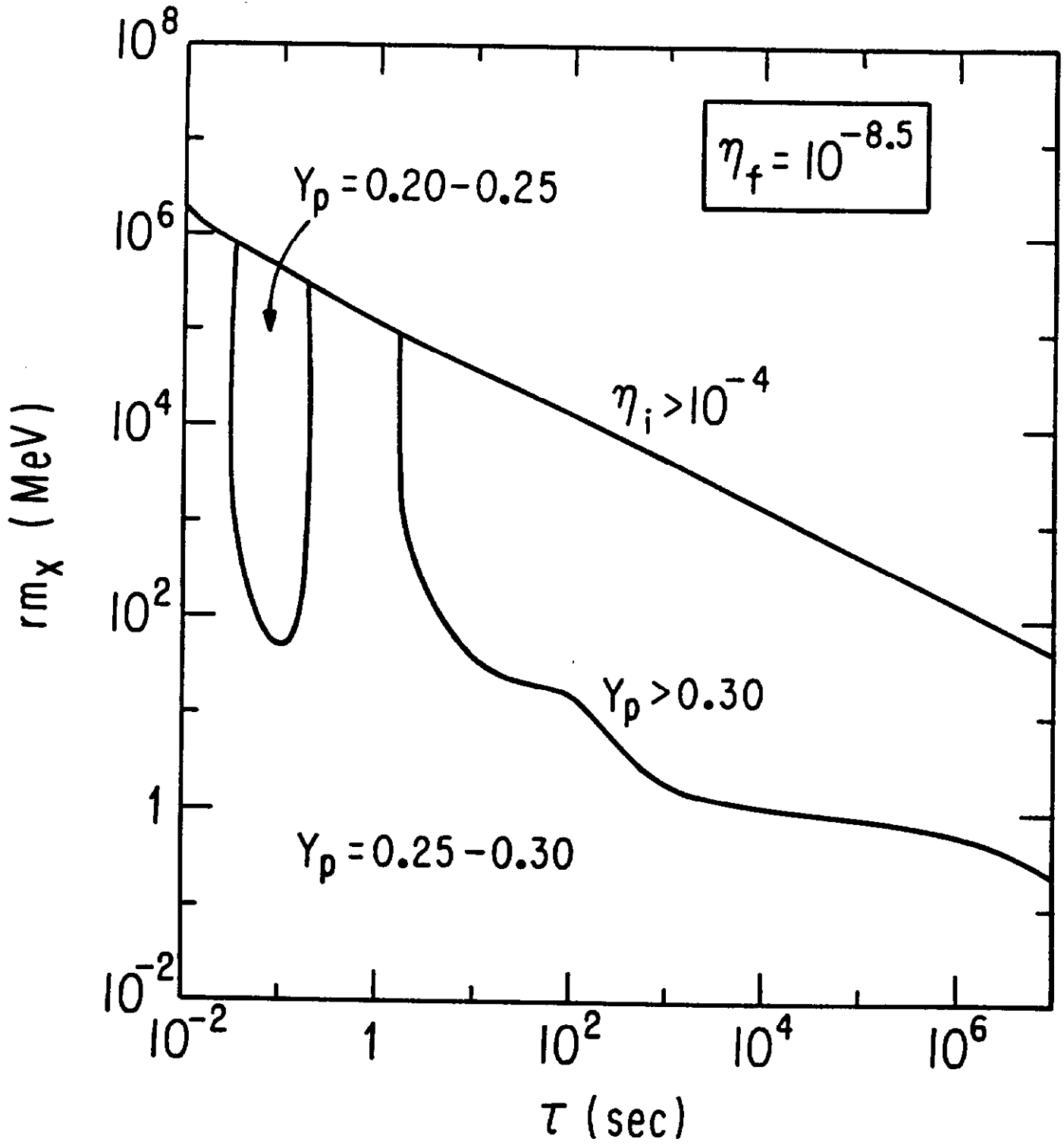


FIG. 7

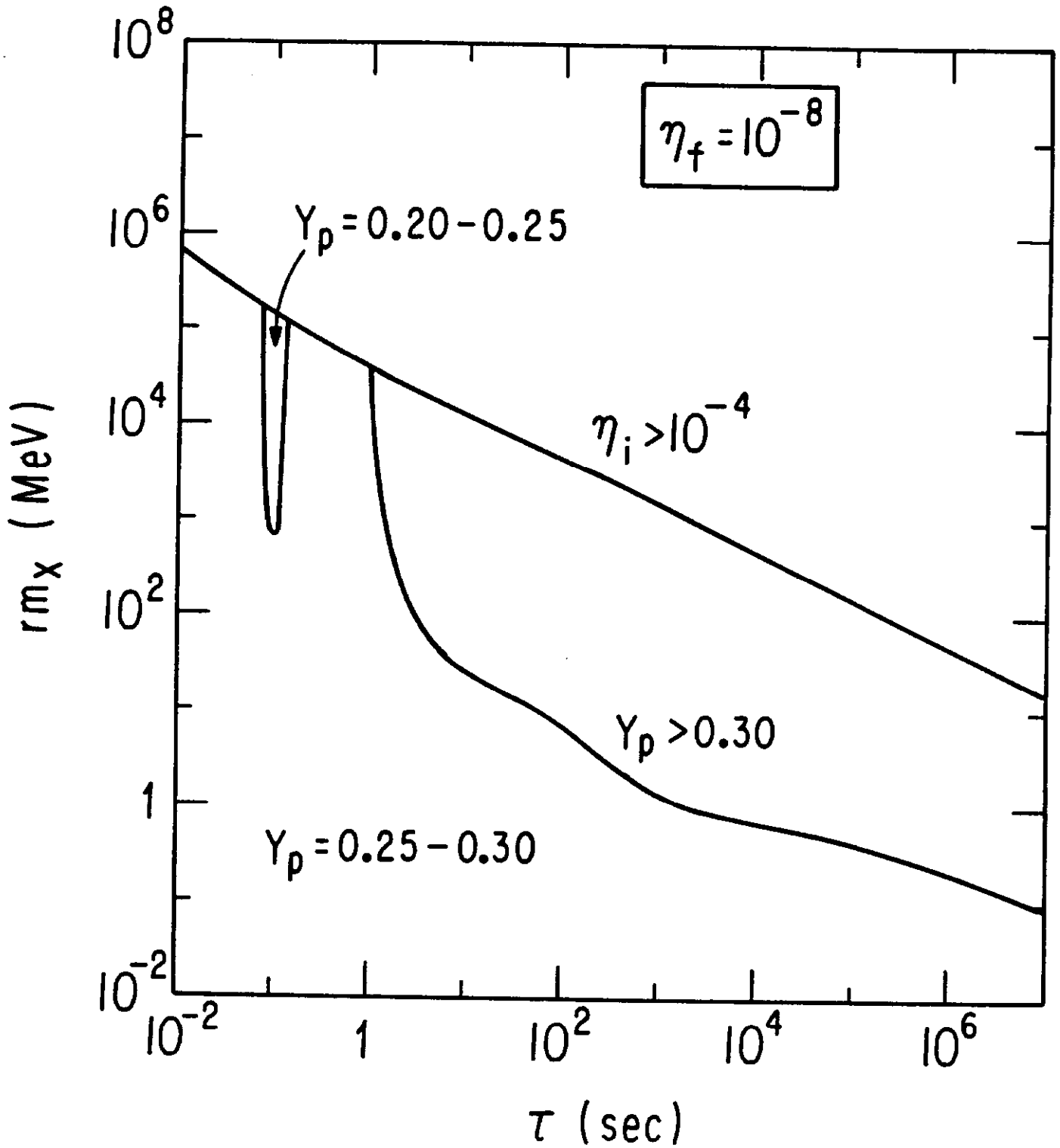


FIG. 8

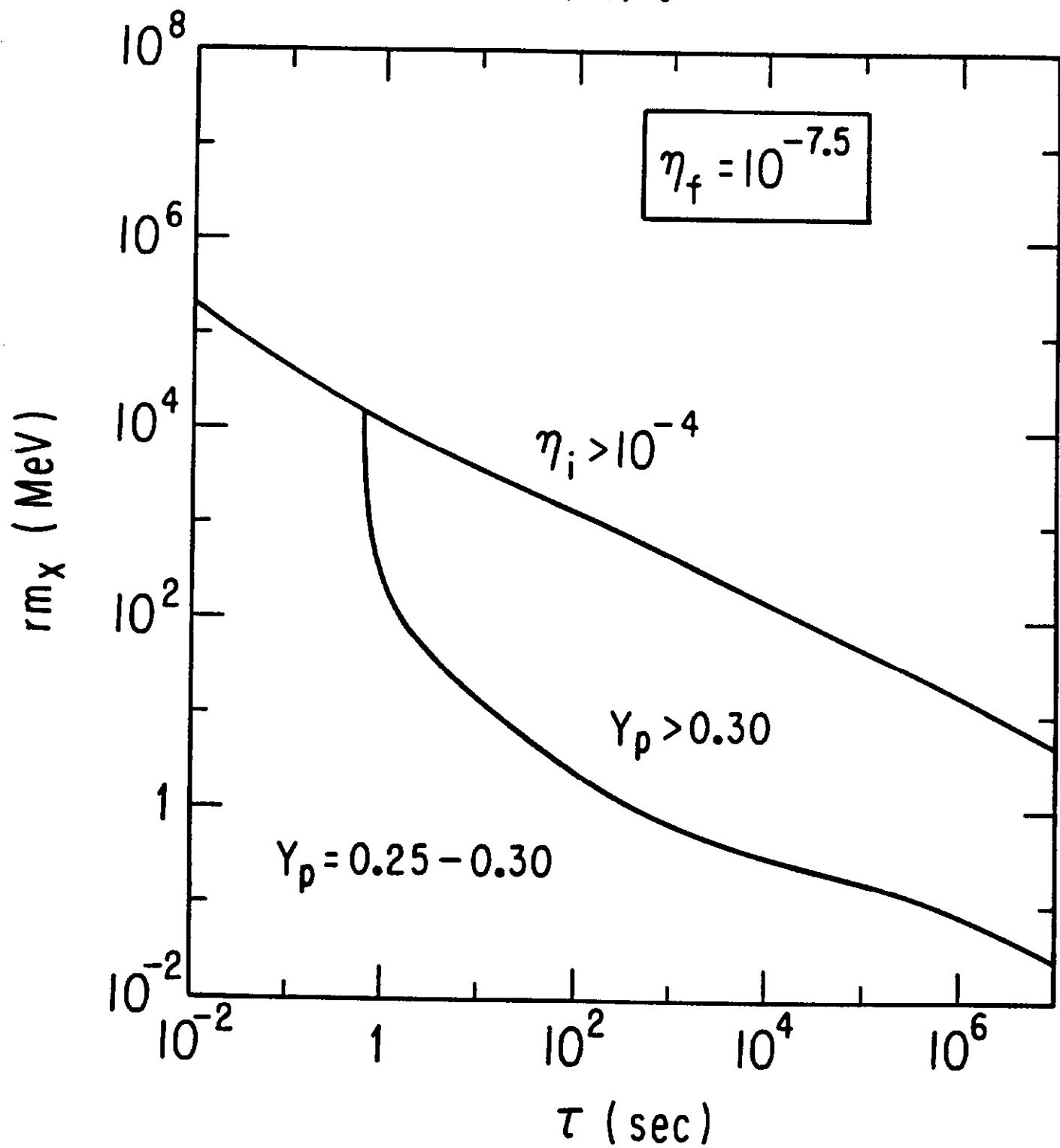


FIG. 9

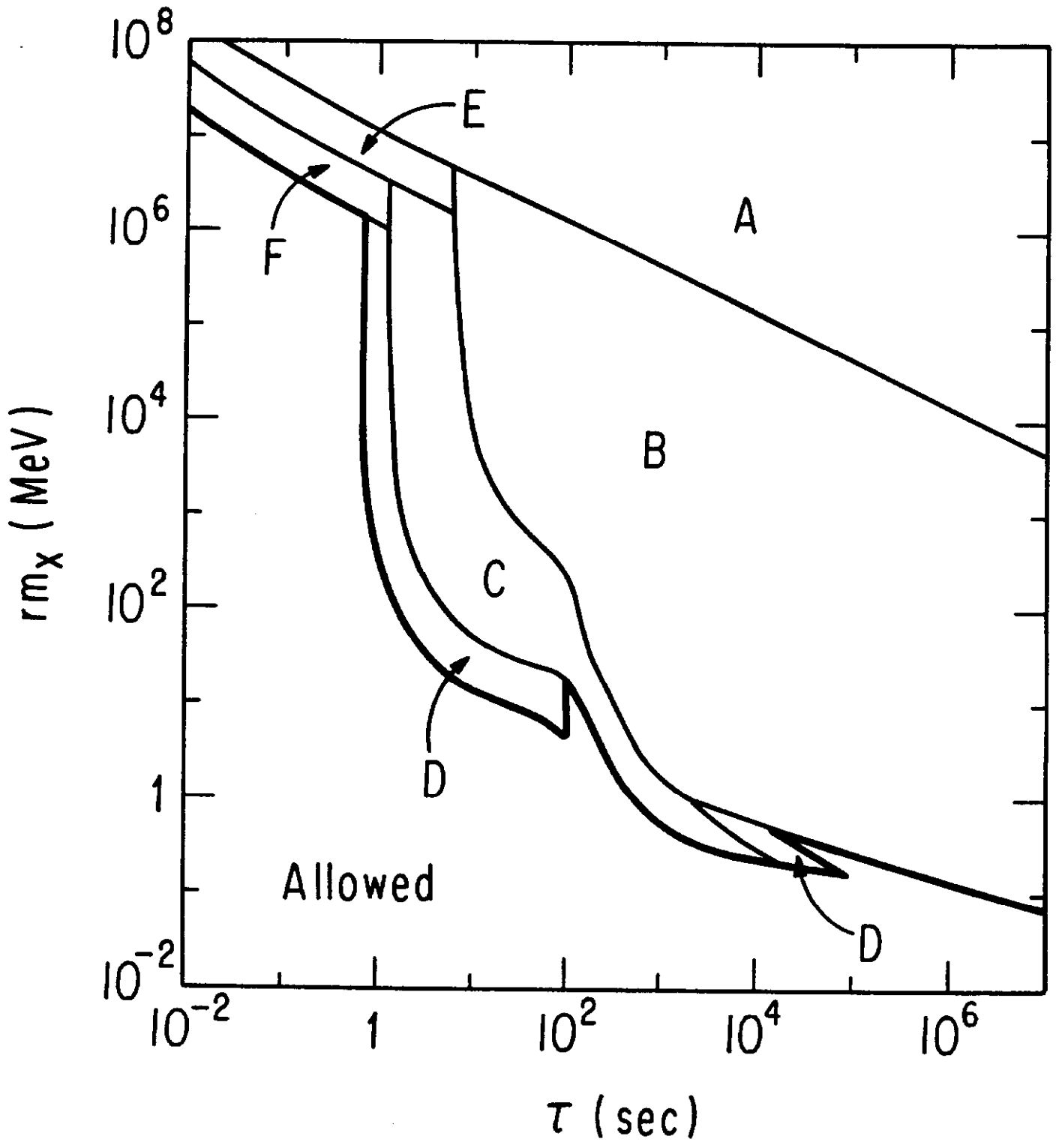


FIG. 10

